0022-3565/11/3392-394–402$25.00
THE JOURNAL OF PHARMACOLOGY AND EXPERIMENTAL THERAPEUTICS
Vol. 339, No. 2
183400/3723361
JPET 339:394–402, 2011
Printed in U.S.A.

The Soluble Guanylate Cyclase Stimulator BAY 41-2272 Inhibits Vascular Smooth Muscle Growth through the cAMP-Dependent Protein Kinase and cGMP-Dependent Protein Kinase Pathways

Chintamani N. Joshi, Danielle N. Martin, Jonathan C. Fox, Natalia N. Mendelev, Trisha A. Brown, and David A. Tulis

Department of Physiology, Brody School of Medicine, East Carolina University, Greenville, North Carolina (C.N.J., D.N.M., J.C.F., T.A.B., D.A.T.); and Department of Pharmaceutical Sciences and Biomanufacturing Research Institute and Technology Enterprise, North Carolina Central University, Durham, North Carolina (N.N.M.)

Received April 27, 2011; accepted August 5, 2011

ABSTRACT

Vascular smooth muscle (VSM) proliferation and migration are key components in vessel remodeling. Cyclic nucleotide signaling is protective and has long-served as a therapeutic target against undesired VSM growth. The present work analyzed the effects of the soluble guanylate cyclase (sGC) stimulator 3-(4-amino-5-cyclopropylpyrimidine-2-yl)-1-(2-fluorobenzyl)-1*H*-pyrazolo[3,4-*b*]pyridine [BAY 41-2272 (BAY)] on VSM growth, and we hypothesize that BAY has the capacity to reduce proliferation and migration via cyclic nucleotide-driven kinase signaling. Perivascular BAY postballoon injury reduced neointimal growth by ~40% compared with vehicle controls after 2 weeks. In VSM cells, BAY (10 μM) reduced proliferation by ~40% after 72 h and migration by ~40% after 6 h and ~60% after 18 h without deleterious effects on cell viability. cGMP content peaked (248×) 20 min after BAY treatment and remained elevated (140×) through 60 min; however, BAY did not affect cAMP levels compared with controls. Conventional and In-Cell Western analyses showed increases in vasodilator-stimulated phosphoprotein (VASP) phosphorylation (pVASP) at serines 239 (3×) and 157 (2×), respective markers of cGMP- and cAMP-directed protein kinases (PKG and PKA, respectively). The PKG inhibitor YGRKKRRQRRRPPLRKKKKKH peptide (DT-2) completely reversed BAY-mediated increases in $pVASPSer_{239}$ and BAY-mediated inhibition of migration. In comparison, the PKA inhibitor peptide PKI further potentiated BAY-stimulated $pVASPSer_{157}$ and $pVASPSer_{239}$ and partially reversed the antiproliferative effects of BAY. This is the first report demonstrating the effectiveness of BAY in reducing neointimal growth with direct evidence for PKG-specific antimigratory and PKA-specific antiproliferative mechanisms. Conclusively, the sGC stimulator BAY reduces VSM growth through cGMP-dependent PKG and PKA processes, providing support for continued evaluation of its clinical utility.

Introduction

Proliferation and migration of vascular smooth muscle (VSM) cells (VSMCs) are key components during the evolution of an atherosclerotic plaque and in the vessel response to injury or intervention. Investigations have attempted to reduce pathologic vessel growth through various interventions including targeted gene delivery (Tulis et al., 2001), the use of drug-coated stents, and localized application of pharmacological agents to the arterial wall (Tulis et al., 2002). Despite advances in genetic and pharmacother-

This study was supported by the National Institutes of Health National Heart, Lung, and Blood Institute [Grants R01-HL081720, R01-HL081720-03S1, R01-HL081720-03S2].

This work was presented previously in poster format: Joshi C, Martin D, Fox C, Adderly S, and Tulis D (2011) Differential regulation of vascular growth through cGMP/PK-G/PK-A signaling, at *Experimental Biology 2011*; 2011 April 9–13; Washington, DC.

Article, publication date, and citation information can be found at http://jpet.aspetjournals.org.

doi:10.1124/jpet.111.183400.

ABBREVIATIONS: VSM, vascular smooth muscle; VSMC, VSM cell; ANOVA, analysis of variance; BAY, BAY 41-2272 [3-(4-amino-5-cyclopropylpyrimidine-2-yl)-1-(2-fluorobenzyl)-1*H*-pyrazolo[3,4-*b*]pyridine]; CA, carotid artery; Cdk, cyclin-dependent kinase; CO, carbon monoxide; DMEM, Dulbecco's modified Eagle's medium; DMSO, dimethyl sulfoxide; DT-2, YGRKKRRQRRRPPLRKKKKKH peptide; FBS, fetal bovine serum; HO, heme oxygenase; IBMX, 3-isobutyl-1-methylxanthine; ICW, In-Cell Western; MW, medial wall; NI, neointima; NO, nitric oxide; NOS, NO synthase; PBS, phosphate-buffered saline; PDE, phosphodiesterase; PDGF, platelet-derived growth factor; PKA, cAMP-dependent protein kinase; PKI, PKA inhibitor; PKG, cGMP-dependent protein kinase; sGC, soluble guanylate cyclase; VASP, vasodilator-stimulated phosphoprotein; pVASP, VASP phosphorylation; pPKASer, phosphorylation of PKA at serine; $VASP_{Tot}$, total VASP; YC-1, 3-(5′-hydroxymethyl-2′-furyl)-1-benzyl indazole.

apy, aberrant VSM growth remains a key contributing factor in vascular pathogenesis, but full characterization of the precise signals involved remains elusive.

Cyclic nucleotide signaling affects numerous homeostatic and pathophysiologic functions in VSM. Carbon monoxide is liberated by the catalytic action of heme oxygenase (HO) on heme, which releases iron and produces the antioxidants bilirubin and biliverdin. Nitric-oxide synthase (NOS) catalyzes conversion of L-arginine to L-citrulline, liberating NO. Binding of CO or NO causes conformational changes in sGC that determines their unique abilities to stimulate the enzyme. Binding of NO causes a 400-fold increase in enzyme activity, whereas CO is able to stimulate the enzyme 4- to 6-fold under controlled conditions (Friebe et al., 1996). Although a relatively poor stimulator compared with NO, CO remains a potent physiological regulator of cGMP-mediated effects in VSM (Liu et al., 2009).

Advances in synthetic, NO-independent sGC stimulators and activators have further established the validity of the CO system to modulate VSM biology. We and others have shown that the sGC stimulator YC-1 [3-(5′-hydroxymethyl-2′-furyl)-1-benzyl indazole] exerts antigrowth effects in VSM under in vivo and in vitro conditions (Tulis et al., 2002; Wu et al., 2004), lending support for CO-directed, cGMP-driven growth suppression. We have investigated 3-(4-amino-5-cyclopropylpyrimidine-2-yl)-1-(2-fluorobenzyl)-1*H*-pyrazolo[3,4-*b*]pyridine [BAY 41-2272 (BAY)], a second-generation YC-1 analog, and found that in rat A7R5 VSMCs BAY stimulates cAMP and cGMP and increases site-specific phosphorylation of vasodilator-stimulated phosphoprotein (VASP) in a manner suggestive of cAMP-dependent protein kinase (PKA) signaling (Mendelev et al., 2009). In this study BAY was also found to exert cytostasis through reduced cyclin-dependent kinase (Cdk) and elevated Cdk inhibitor expression. In addition, BAY has been reported to possess antihypertensive and antiplatelet effects (Boerrigter et al., 2003), making it an attractive agent for further study to target cardiovascular disorders.

cAMP and cGMP activate PKA and PKG, respectively, leading to phosphorylation of key regulatory proteins, including VASP, which plays important roles in controlling cytoskeleton dynamics and cell migration (Reinhard et al., 2001). In platelets, VSMCs, and vascular endothelial cells VASP is associated with actin filaments, focal adhesions, and cell-cell contacts. VASP can be phosphorylated on three sites: serine 157 (a PKA-preferred site), serine 239 (a PKG-preferred site), and threonine 278 (an AMP kinase-activated site) (Butt et al., 1994; Reinhard et al., 2001). $VASPSer_{157}$ has also been shown to be phosphorylated in response to growth factors activated by protein kinase C (Chitaley et al., 2004). Although VASP phosphorylation is often used as a biochemical marker for activation of PKG and PKA, it possesses important cellular and molecular functions that have yet to be fully elucidated in VSM.

In VSMCs, cGMP-driven PKG has been shown to modulate apoptosis, proliferation, (Chiche et al., 1998), migration (Boerth et al., 1997), and extracellular matrix protein expression (Reinhard et al., 2001), suggesting involvement in normal cellular homeostasis. In the current study, we investigated the influence of BAY-induced cGMP signaling in VSM growth in vivo and in vitro, using $VASPSer_{157}$ and $VASPSer_{239}$ as readouts for respective PKA or PKG and as functional mediators of growth. Our a priori hypothesis is that BAY serves to reduce VSM growth through reduction in proliferation and migration and via mechanisms involving cyclic nucleotide-driven kinases. Results show that BAY reduces proliferation and migration of primary VSM through the actions of cGMP/PKA and cGMP/PKG/$VASPSer_{239}$, respectively. These findings provide the first evidence for BAY in limiting VSM growth and that cGMP has the capacity to influence distinct downstream targets (PKA, PKG, phosphoVASP), resulting in discrete regulation of VSM growth.

Materials and Methods

This study abided by the guidelines of the Institutional Animal Care and Use Committee and conformed to the *Guide for the Care and Use of Laboratory Animals* (Institute of Laboratory Animal Resources, 1996).

Rat Carotid Artery Balloon Injury Model. The in vivo arterial response to injury was studied using the highly characterized rat carotid artery (CA) model of balloon injury (Tulis, 2007a). In brief, male Sprague-Dawley rats (Harlan, Indianapolis, IN) weighing 450 to 550 g were anesthetized with a combination anesthetic (ketamine, 90 mg/ml; xylazine, 10 mg/ml; 1 ml/kg i.p.) and provided buprenorphine (Buprenex; 0.5 ml/kg s.c.) supplied by the Department of Comparative Medicine, Brody School of Medicine, East Carolina University, Greenville, NC. The left common CA and external carotid branch were exposed, and a Fogarty 2F embolectomy catheter (Baxter Healthcare Corp., Irvine, CA) was introduced into the external carotid branch through an arteriotomy and advanced uninflated to the aortic arch. The balloon was inflated to 2 atm (0.02 ml) and withdrawn three times with rotation. The catheter was removed and the external carotid artery was ligated. Vessel patency and CA blood flow were verified, overlying tissue was sutured, and the skin was closed with rodent wound clips. After full recovery from anesthesia, animals were returned to the animal care facility and provided standard rat chow and water ad libitum.

BAY 41-2272. Following established protocols for topical application of pharmacologic agents to carotid vasculature (Tulis, 2007a), BAY 41-2272 (1 mg; Enzo Life Sciences, Inc., Farmingdale, NY) was dissolved in 50 μl of DMSO (Calbiochem, San Diego, CA) and mixed into 200 μl of a 25% solution of a copolymer gel (Pluronic F-127; BASF Corporation, Mount Olive, NJ). Immediately after balloon injury and closure of the external carotid arteriotomy, the BAY-Pluronic F-127 gel mixture was administered topically and circumferentially on the exposed adventitia of the CA section. Control animals were treated with 200 μl of gel containing 50 μl of DMSO. The right CA served as the unmanipulated untreated control.

Tissue Processing and Staining. Following protocols for histology of rat vascular tissues (Tulis, 2007b), 2 weeks after injury rats were sacrificed by an anesthetic overdose followed by pneumothorax and exsanguination. The thoracic artery was clamped and normal saline was perfused transcardially followed by 10% buffered formalin in PBS. Carotid arteries were harvested, postfixed, and processed in graded alcohols and aliphatic xylene substitute (VWR, West Chester, PA) and embedded in paraffin. For elastin staining, slides were deparaffinized, rehydrated, and stained with elastic staining solution containing alcoholic hematoxylin, ferric chloride, and Weigert's iodine. Slides were differentiated in ferric chloride and Van Gieson-counterstained. Images were captured microscopically (Leica DM5000B; Leica, Wetzlar, Germany) and analyzed using Image Pro Plus 6.3 software (Media Cybernetics, Inc., Bethesda, MD).

Rat Primary VSMC Cultures. VSMCs were isolated from the thoracic aorta of male Sprague-Dawley rats (100–125 g) by collagenase and elastase digestion (Tulis et al., 2002; Liu et al., 2009). Cells were cultured serially (passages 1–6) in Dulbecco's minimum Eagle's media (DMEM) supplemented with 10% fetal bovine serum (FBS), 2 mM L-glutamine, sodium pyruvate, 5 mM HEPES and Primocin (100 mg/l) in the presence of 95% air/5% CO_2.

cGMP and cAMP Assays. Primary VSMCs were grown in 24-well plates (60,000 cells/well), and cyclic nucleotide enzyme-linked immunosorbent assay-based assays (Sigma, St. Louis, MO) were performed according to the manufacturer's guidelines. In brief, after pretreatment with IBMX (1 mM; 15 min), cells were incubated in the presence of BAY for specific times, after which cyclic nucleotides were extracted in 0.1 M HCl and their contents were estimated. Protein was determined using the BCA protein assay (Thermo Fisher Scientific, Waltham, MA), and cyclic nucleotide content was normalized to total protein within each sample.

VSMC Proliferation. VSMCs were seeded in 48-well plates (25,000 cells/well), and after adherence they were quiesced overnight in 0.2% FBS. Cells were treated with either vehicle (DMSO in DMEM) or BAY (0.001, 0.1, or 10 μM in DMSO/DMEM) for 72 h. For the kinase inhibitor studies, cells were incubated in the presence or absence of BAY (10 μM) along with the PKG inhibitor YGRKKRRQRRRPPLRKKKKKH peptide (DT-2) (10 μM in DMSO/DMEM) (Dey et al., 2005) or the PKA inhibitor (PKI) (1 μM in DMSO/DMEM) (Schlegel and Waschke, 2009) for 72 h. Cells in each well were then trypsinized individually (0.25% trypsin, 5 min, 37°C), and cell counts were estimated using hemocytometry.

Cell Cycle Analysis. Flow cytometry was performed as routine. In brief, VSMCs were seeded in 48-well plates (30,000 cells/well), and after adherence they were quiesced overnight in 0.2% FBS containing DMEM. Cells were then treated with vehicle or BAY (10 μM), and after 24 h cells were trypsinized, fixed in cold ethanol, stained with propidium iodide, and subjected to flow cytometry (Accuri C6; Accuri Cytometers Inc., Ann Arbor, MI).

Neutral Red Uptake. To evaluate cellular viability and cytotoxicity of BAY, the neutral red uptake assay was performed with minor modifications. In brief, VSMCs were seeded in 96-well plates (18,000 cells/well) and grown for 24 h. Cells were then incubated in the presence of vehicle or BAY (10 μM) for 18 h, after which treatments were replaced with neutral red solution in complete media and incubated at 37°C for 3 h. Cells were washed with warm PBS and neutral red was extracted using 200 μl/well acetic ethanol solution. Extracts (150 μl) from each well were transferred to new 96-well plates and read at 540 nm.

Migration Assays. Two standardized assays were used to estimate cell migration. Nonspecific migration was assessed using an in vitro scrape injury model (Yang et al., 2006). In brief, VSMCs were seeded in 24-well plates (75,000 cells/well) and grown to confluence. A cell scraper was fabricated to approximately 1-mm width. Cells were pretreated with respective BAY concentrations (1 nM-10 μM) for 20 min. A portion of the cell layer was then denuded via scraping, after which cells were washed with PBS and incubated in vehicle/BAY treatments in complete media. The scraped regions were photographed immediately after injury (time 0) and after 18, 24, and 42 h under an inverted microscope (Leica DMI4000B). Using a micrometer scale the images were calibrated, and the distances between the edges of the scrape were measured (between six and eight measurements per well). The extent of VSMC migration in the presence of vehicle and BAY at 18, 24, or 42 h was calculated relative to time 0, and the scrape injury distance for each respective well was calculated. The BAY treatments were then normalized to vehicle controls and percentage of regrowth was determined.

A transwell chemotactic migration assay was also performed (Yang et al., 2006). In brief, VSMCs (9000–18,000) were seeded on membrane inserts (Costar Transwell; Corning Life Sciences, Lowell, MA; 8.0-μm pores; 6.4-mm diameter) in complete DMEM, with the bottom part of the well containing only DMEM. After adherence, media in the top portion of the insert were replaced with vehicle or BAY with/without the PKA and PKG inhibitors PKI and DT-2, respectively, in DMSO/DMEM. The inhibitors were added 15 min before BAY treatment. The chemoattractant PDGF (2 ng/ml) was added to the bottom portions of the wells after 15 min of vehicle/drug treatment. After 6 h the top portion of the insert was cleaned with a cotton Q-tip and the media in the bottom part of the well were replaced with 4% buffered formalin solution to fix the cells for 20 min. The migrated cells on the bottom part of the inserts were stained with hematoxylin solution. Within each insert, six fields were counted under light microscopy. Each treatment set was normalized to its respective vehicle control from the same plate and presented as percentage of migration.

Western Blotting. Traditional Western blotting was performed on whole-cell lysates (Mendelev et al., 2009) with slight modifications. After treatment, cells were collected, homogenized, sonicated, and boiled, and SDS-polyacrylamide gel electrophoresis was performed using 20 μg of protein samples. The separated blots were transferred to nitrocellulose membrane, blocked, and incubated with antibodies directed against VASP, pVASPSer$_{157}$, pVASPSer$_{239}$ (Cell Signaling Technology, Danvers, MA), PKA, PKG (Abcam Inc., Cambridge, MA), and pPKASer$_{338}$ (Biosource International, Camarillo, CA), all at 1:1000 dilution and incubated overnight at 4°C. After washes the membranes were incubated in anti-rabbit horseradish peroxidase-conjugated secondary antibodies (1:1000) for 1 h at room temperature. Blots were washed and incubated in Pierce enhanced chemiluminescence reagents (Thermo Fisher Scientific) and exposed to photographic film. Densitometry was performed using ImageJ 1.42q software (National Institutes of Health, Bethesda, MD). The blots were stripped of the antibodies at 50°C for 30 min using a stripping solution containing 10% SDS and 100 mM 2-mercaptoethanol in 62.5 mM Tris buffer, pH 6.8, before reprobing for complementary proteins.

In-Cell Western Assays. The In-Cell Western (ICW) method was used on intact adherent cells to study phosphorylation events stimulated by BAY alone or in the presence of PKA and PKG inhibitors (Chen et al., 2005). Primary VSMCs were seeded in black 96-well, flat-bottom plates (22,000 cells/well) and, after attachment, treated with BAY (10 μM) with or without the PKA and PKG inhibitors PKI or DT-2 (each at 5 and 10 μM) using appropriate vehicle controls for a total incubation time of 60 min. Reactions were stopped by replacing media with 4% phosphate-buffered formalin. Fixed cells were permeabilized with 0.1% Triton X-100, blocked, and incubated with rabbit antibodies against total VASP or the phosphorylated forms of VASP at serines 157 or 239 (Cell Signaling Technology) along with mouse α-tubulin (Sigma) as the housekeeping control at 1:500 dilutions overnight at 4°C. The cells were washed with PBS-Tween and incubated with anti-rabbit IR 800 and anti-mouse IR 680 (Rockland Immunochemicals, Gilbertsville, PA) secondary antibodies for 1 h. The proteins were quantified by fluorescence (LI-COR Odyssey; LI-COR Biosciences, Lincoln, NE) and normalized with respect to α-tubulin within each well.

Statistical Analyses. Data were analyzed using Excel 2007 (Microsoft, Redmond, WA) and Sigma Plot 11 (SPSS, Inc., Chicago, IL). Comparisons between treatment groups were made using one-way analysis of variance (ANOVA) and a multiple comparison Newman-Keuls post hoc test or Student's t test as indicated. All data are presented mean ± S.E.M. A p value of <0.05 is considered statistically significant for all comparisons.

Results

Rat Carotid Artery Balloon Injury Model. Perivascular treatment of rat carotid arteries with BAY immediately after balloon injury significantly reduced neointimal (NI) growth compared with vehicle-treated arteries 2 weeks after injury. Representative photomicrographs (400×) of balloon-injured, perfusion-fixed left CA cross-sections of vehicle- and BAY-treated vessels are shown in Fig. 1, A and B, respectively. Morphometric analyses show that the NI area was reduced ~40% ($p < 0.01$) (Fig. 1C) and the NI/medial wall (MW) area ratio was reduced ~50% ($p < 0.05$) in BAY-treated vessels compared with vehicle controls (Fig. 1D). Significant differences in arterial MW areas were not de-

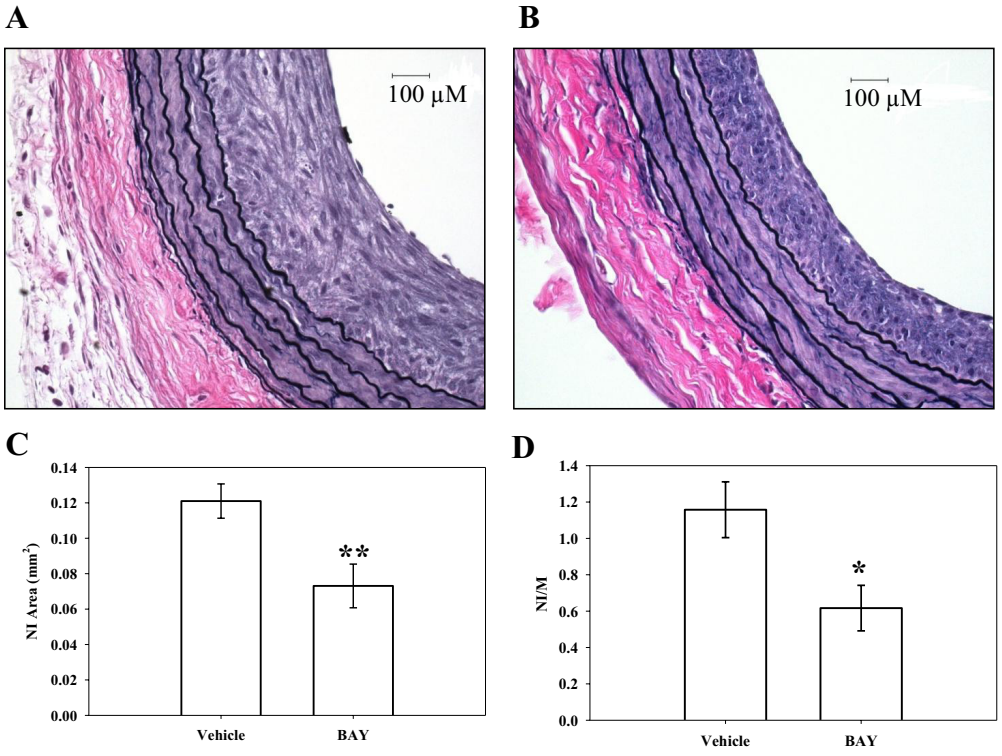

Fig. 1. Representative photomicrographs (400×) of balloon-injured, perfusion-fixed rat carotid artery cross-sections 2 weeks postinjury. A, Pluronic F-127 gel with vehicle (n = 6). B, Pluronic F-127 gel containing BAY (n = 7). C and D, morphometric analyses indicate that BAY significantly reduces NI area (~40%; $p < 0.01$) (C) and significantly reduces the NI to MW area ratio (~50%; $p < 0.05$) (D) compared with vehicle (DMSO in Pluronic F127 gel) controls. *, $p < 0.05$; **, $p < 0.01$ compared with vehicle-treated control vessels.

tected between BAY-treated (0.1087 ± 0.0049 mm^2) and vehicle-treated (0.1082 ± 0.0055 mm^2) injured arteries 2 weeks postinjury. Likewise, significant differences were not detected in adventitial areas between BAY-treated (0.179 ± 0.018 mm^2) and vehicle-treated (0.2079 ± 0.043 mm^2) injured arteries after 2 weeks. Lengths of the external and internal elastic lamina were also not different between BAY- and vehicle-treated injured vessels at this time point (external elastic lamina, 2.68 ± 0.039 versus 2.61 ± 0.08; internal elastic lamina, 2.40 ± 0.03 versus 2.32 ± 0.07, respectively).

Rat Primary VSMC Culture Studies. Using hemocytometry, BAY (10 μM) reduced FBS-stimulated VSMC numbers by ~40% ($p < 0.01$) compared with vehicle-treated controls after 72 h (Fig. 2). Lower concentrations of BAY also reduced cell numbers by ~20% (0.001 μM BAY, p = 0.196; 0.1 μM BAY, p = 0.165) at this time point. Using flow cytometry, a trend for reduced cell numbers in the G_2/M phase (−70%; not statistically significant; p = 0.091) in BAY (10 μM)-treated cells compared with vehicle controls is apparent with only a slight (nonsignificant) increase in the number of cells in G_0/G_1 after 24 h (Fig. 3). No differences were observed between vehicle- and BAY-treated cells in the S phase at this time point. Using the neutral red uptake assay as an indicator of cellular toxicity, no differences be-

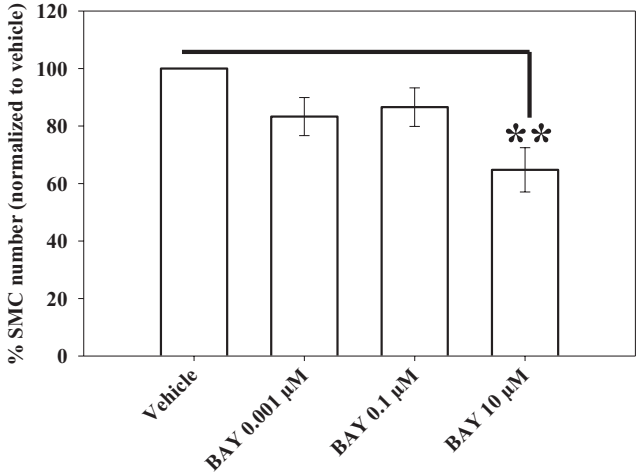

Fig. 2. Effects of BAY on 10% FBS-stimulated VSMC numbers. At 10 μM, BAY significantly ($p < 0.01$) reduces cell numbers by ~35% after 72 h compared with vehicle controls. No changes in cellular toxicity from BAY were observed using the neutral red assay (data not shown). Data are mean ± S.E.M. of three independent experiments (each n = 6). Student-Newman-Keuls method for multiple comparisons after one-way ANOVA was used. **, $p < 0.01$ compared with normalized vehicle controls.

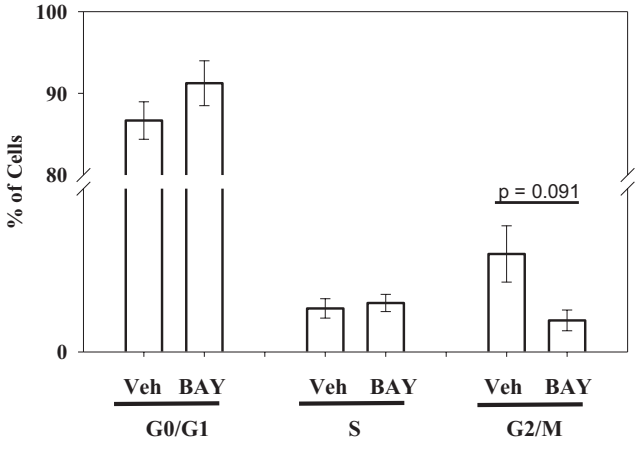

Fig. 3. Effect of BAY on VSMC cycle progression. Histogram of propidium iodide-labeled DNA content for vehicle (Veh)- and BAY-treated cells after 24 h in the presence of 10% FBS. A trend for reduced cell numbers in G_2/M with BAY treatment is apparent (−70%; not statistically significant; p = 0.091), whereas the number of cells in the G_0/G_1 stationary phase is slightly increased. No significant effects by BAY were observed on the numbers of cells in the S phase. Data are mean ± S.E.M. of three independent experiments (each n = 6 per group).

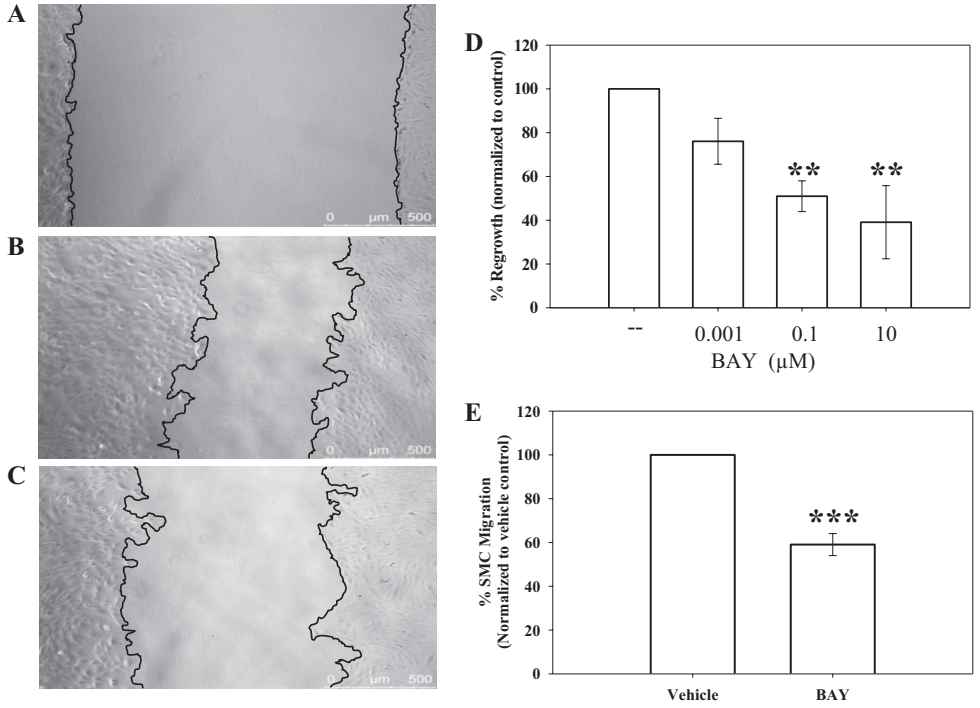

Fig. 4. VSMC migration assays. A to C, representative photomicrographs of scrape-injured confluent cells showing borders of denuded regions. A, vehicle-treated control at time 0. B, vehicle-treated cells after 18 h. C, BAY (10 μM)-treated cells after 18 h. BAY significantly reduced 10% FBS-stimulated VSMC migration after scrape injury after 18 h at both 0.1 μM (50%) and 10 μM (60%). D, data showing inhibition of VSMC migration by BAY after scrape injury and stimulation by 10% FBS. Percentage of regrowth after injury was calculated after normalizing readouts to time 0 controls. E, migration was measured using the transwell method with PDGF (20 ng/ml) stimulation after 6 h. BAY significantly reduced (~50%) chemotaxis after 6 h compared with vehicle controls. Data are mean ± S.E.M., with $n = 3$ for both assays, each performed in duplicate. **, $p < 0.01$; ***, $p < 0.001$, Student-Newman-Keuls method for multiple comparisons after one-way ANOVA was used.

tween BAY-treated (0.37 ± 0.005), vehicle (DMSO)-treated (0.34 ± 0.009), and DMEM control (0.36 ± 0.01) cells were observed after 18 h.

Figure 4 shows the results of studies examining the effects of BAY on cell migration. Using a scrape injury method, at 18 h postscraping BAY significantly inhibited FBS (10%)-stimulated cell migration at both 0.1 μM (50% decrease; $p < 0.01$) and 10 μM (60% decrease; $p < 0.01$) compared with cells in the presence of vehicle alone (Fig. 4D). Representative photomicrographs are shown for VSMCs immediately after scraping at time 0 (Fig. 4A), 18 h after scraping in the presence of vehicle (DMSO in DMEM) (Fig. 4B), and 18 h after scraping in the presence of 10 μM BAY (Fig. 4C). Significant reduction in VSMC migration by BAY was also observed with the scrape injury after 24 h (data not shown); however, by 42 h after scraping, the extent of regrowth was similar for cells in vehicle and BAY treatments at all concentrations (data not shown). In complement, migration of VSMCs was measured using a modified transwell migration system with PDGF as a chemoattractant. After 6 h in the presence of PDGF (20 ng/ml), VSMC migration was reduced by ~40% ($p < 0.001$) compared with vehicle controls (Fig. 4E).

Regarding signaling events mediated by BAY, in the presence of the broad PDE inhibitor IBMX BAY (10 μM) increased cGMP content more than 200-fold ($p < 0.001$) within 20 min, which remained elevated through 60 min (~140-fold; $p < 0.001$) compared with vehicle controls (Fig. 5). In the presence of IBMX, no differences were observed in cAMP content between BAY-treated VSMCs (10 μM) and vehicle controls at any time point within 60 min (data not shown).

Considering its novelty, initial studies examined the effectiveness and reproducibility of ICW blotting to that of standardized Western blotting. Using ICW and normalizing to α-tubulin within each well, VSMCs in the presence of BAY (10 μM; 60 min) doubled $pVASPSer_{157}$ and tripled $pVASPSer_{239}$ compared with vehicle controls (Fig. 6, A and B, respectively). The same

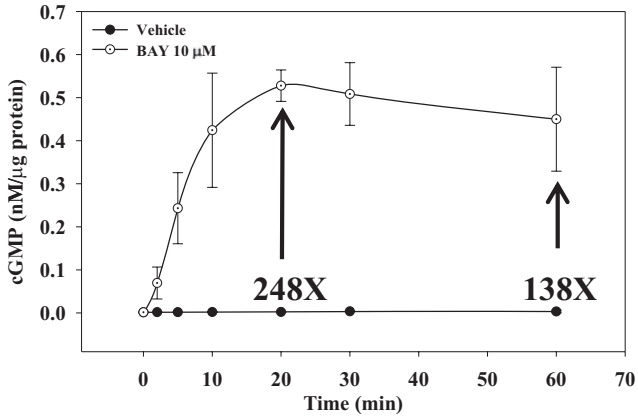

Fig. 5. Time-dependent increases in cGMP content in VSMCs stimulated with BAY (10 μM). The levels of cGMP peaked at 20 min after BAY treatment, reaching levels ~250 times over that of vehicle-treated cells. These levels of cGMP persisted through 60 min (~140×) compared with controls. No differences between BAY and vehicle groups were observed for cAMP levels at any time point ≤60 min (data not shown). Data are mean ± S.E.M. from two independent experiments performed in duplicate.

experimental scheme (including α-tubulin normalization) was then used with conventional Western blotting, and results show comparable and dose-dependent up-regulation of both $pVASPSer_{157}$ and $pVASPSer_{239}$ with BAY (Fig. 6C). Analyses for α-tubulin alone also revealed consistent and reproducible expression patterns from ICW and traditional Western blotting (data not shown).

Using site-specific phosphorylation of VASP as a marker for kinase-specific activation, with $pVASPSer_{157}$ suggestive of active PKA and $pVASPSer_{239}$ indicative of active PKG (Butt et al., 1994; Deguchi et al., 2002; Chen et al., 2004) in the current study BAY (0.1–10 μM, 60 min) dose-dependently increased both $pVASPSer_{157}$ and $pVASPSer_{239}$ (Fig. 6C). Increases in $pVASPSer_{157}$ and $pVASPSer_{239}$ by BAY

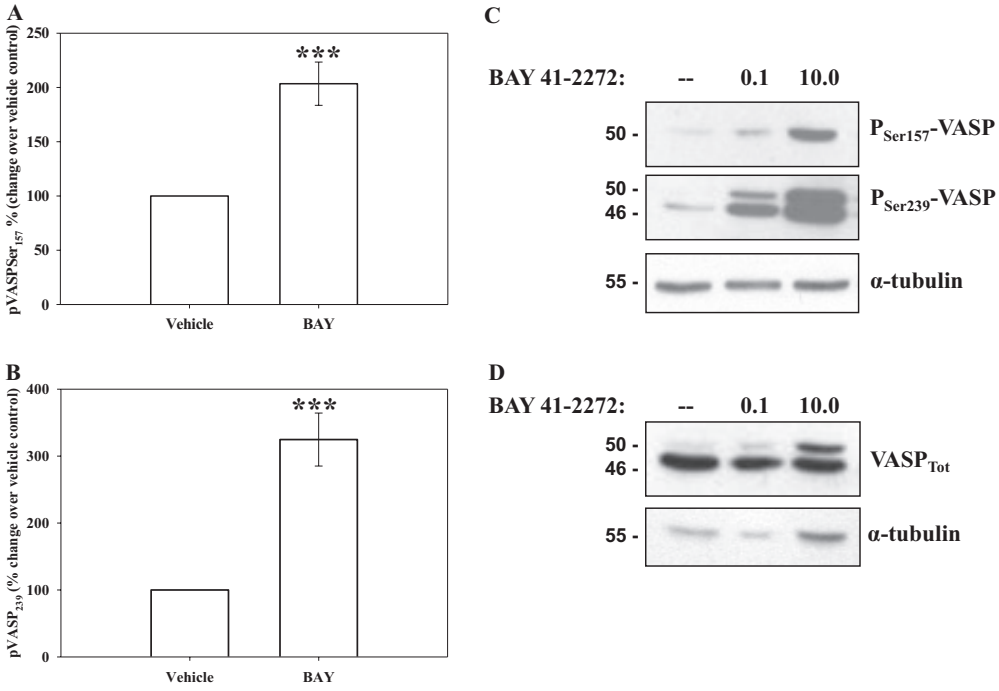

Fig. 6. The presence of BAY (10 μM, 60 min) stimulated phosphorylation of VASP at Ser_{157} and Ser_{239} detected by In-Cell and traditional Western blotting. A, the stimulation at $pVASPSer_{157}$ is doubled ($p < 0.001$) compared with vehicle controls. B, stimulation of $pVASPSer_{239}$ is tripled ($p < 0.001$) compared with vehicle controls. Data are mean ± S.E.M. of three independent experiments each performed in triplicate. ***, $p < 0.001$. C and D, representative images of Western blotting showing concentration-dependent increases in VASP phosphorylation at both Ser_{157} and Ser_{239} after BAY treatment (0.1–10 μM; 24 h) compared with the vehicle controls (C) and increases in total VASP content ($VASP_{Tot}$) after BAY treatment (0.1–10 μM; 24 h) (D).

(0.001–10.0 μM; 60 min; normalized to α-tubulin) were also observed in rat intact carotid arteries ex vivo (data not shown). In separate sets of ICW and traditional Western blotting experiments, VSMCs were treated with BAY, and total VASP (normalized to α-tubulin) was quantitated. Figure 6D shows a representative Western blot, and total VASP ($VASP_{Tot}$) including both upper (phosphorylated) and lower (unphosphorylated) bands is only marginally increased in response to BAY (10 μM; 24 h) compared with vehicle controls; nonetheless, a dose-dependent increase (8-fold at 10 μM BAY) in the levels of phosphorylated (not site-specific) VASP (upper band) normalized to $VASP_{Tot}$ (both bands) is clear. Expression of total PKA and total PKG were not different in BAY-treated cells or BAY-treated intact carotid arteries compared with vehicle controls over a range of BAY concentrations and time points (data not shown). The influence of BAY on site-specific phosphorylation of PKA at serine 338 ($pPKASer_{338}$) a reported indicator of PKA catalytic activity (Yonemoto et al., 1993), was also evaluated, and results show a marked increase in $pPKASer_{338}$ in BAY-treated cells compared with vehicle controls (data not shown).

Regarding kinase pathways involved in BAY-driven signaling, the PKA inhibitor PKI (Han et al., 2006) and the PKG inhibitor DT-2 (Dey et al., 2005) have been verified when using VASP phosphorylation as the endpoint (Profirovic et al., 2005; Koika et al., 2010). The PKG inhibitor DT-2 (10 μM) did not significantly reduce BAY-stimulated $pVASPSer_{157}$ (~20%; $p = 0.14$) (Fig. 7A). It is noteworthy that the PKA inhibitor PKI (10 μM) further stimulated BAY-induced $pVASPSer_{157}$ by ~30% ($p = 0.03$) compared with BAY alone (Fig. 7A). In comparison, inhibition of PKG by DT-2 completely eliminated BAY-induced stimulation of $pVASPSer_{239}$ (Fig. 7B); however, surprisingly, again PKI further increased BAY-stimulated $pVASPSer_{239}$ by ~50% ($p = 0.03$) compared with effects of BAY alone (Fig. 7B). Slight increases in both $pVASPSer_{239}$ ($p = 0.104$) and $pVASPSer_{157}$ ($p = 0.101$) were also observed with 5 μM PKI compared with the BAY-treated group (data not shown). The inhibition of PKG by DT-2 even at a lower concentration (5 μM) almost completely

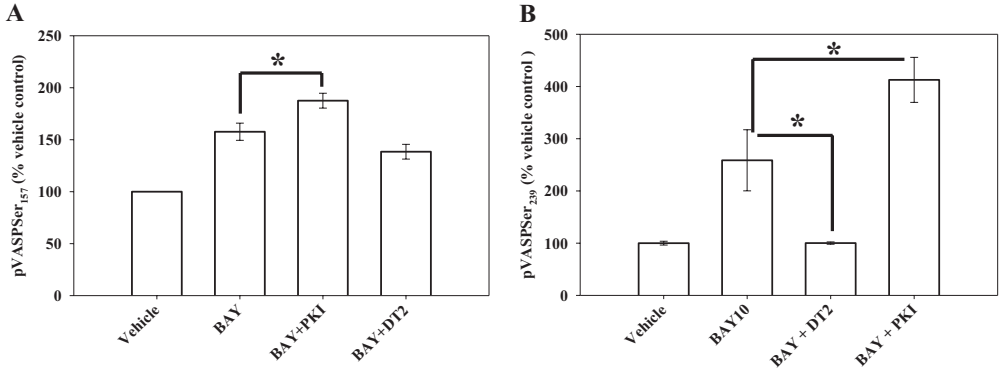

Fig. 7. Site-specific VASP phosphorylation by BAY: roles of PKA versus PKG signaling. A, using $pVASPSer_{157}$ as a readout for PKA activity, increased expression of $pVASPSer_{157}$ by BAY is further enhanced with the PKA inhibitor PKI, whereas the PKG inhibitor DT-2 failed to exert noticeable changes. B, using $pVASPSer_{239}$ as readout for PKG activity, inhibition of PKG by DT-2 completely reversed BAY stimulation of $pVASPSer_{239}$, but PKA inhibition by PKI again further increased the levels of $pVASPSer_{239}$ compared with BAY alone. Data are mean ± S.E.M. $n = 3$ per treatment group. *, $p < 0.05$; Student-Newman-Keuls method for multiple comparisons after one-way ANOVA.

inhibited BAY-stimulated pVASPSer$_{239}$ ($p = 0.026$) but only marginally reduced pVASPSer$_{157}$ ($p = 0.19$) (data not shown).

Considering the kinase signaling pathways involved in growth inhibition by BAY, DT-2 (10 μM) did not influence the antiproliferative actions of BAY in VSMCs after 72 h, yet PKI (1 μM) partially ($p = 0.369$) restored the effects of BAY toward control numbers (Fig. 8). These experiments were conducted over 72 h, so a lower dose of PKI (1 μM) was used to avoid unwanted influence from prolonged exposure. Regarding migration, coincubation of VSMCs with BAY and DT-2 completely reversed BAY-mediated inhibition of migration ($p < 0.001$); conversely, PKI had no effect on the antimigratory effects of BAY (Fig. 9).

Discussion

During atherogenesis and after vascular intervention, dysfunction of intimal endothelium can occur concomitant with conversion of medial VSMCs to a growth-promoting, embryonic phenotype. Under such conditions endothelial NOS signaling is often perturbed, yet a compensatory mechanism exists in HO-mediated CO generation. We have shown that under inimical conditions, HO/CO-stimulated cGMP has the capacity to elicit growth-retarding effects in VSM (Tulis et al., 2001). This study and others (Chiche et al., 1998) have identified bioactivity of the HO/CO/cGMP system to evoke protection against VSM growth through vasodilatory, antiinflammatory, and antimitogenic activities. Further evidence for the salutary impact of HO/CO-mediated signaling on VSM function can be found in studies using the sGC stimulator YC-1 (Tulis et al., 2002; Wu et al., 2004), which helped validate the antiproliferative influence of this system on VSM growth.

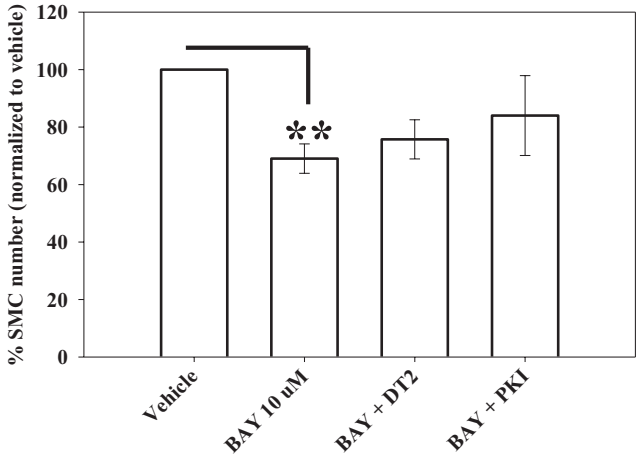

Fig. 8. The reduction in VSMC numbers by BAY (10 μM; 72 h) is partially reversed by the PKA-specific inhibitor PKI, whereas the PKG inhibitor DT-2 failed to exert effects. Data are mean ± S.E.M. of three independent experiments performed in triplicate. **, $p < 0.01$; Student-Newman-Keuls method for multiple comparisons after one-way ANOVA.

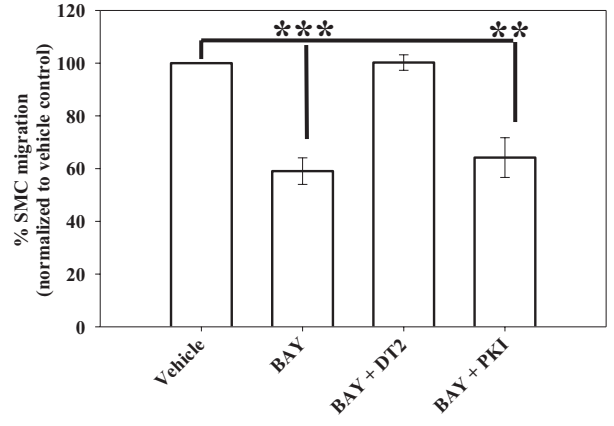

Fig. 9. The presence of BAY significantly reduced (40%) PDGF-stimulated migration of VSMCs after 6 h using a transwell assay. The PKG inhibitor DT-2 completely reversed the antimigratory effects of BAY, whereas the PKA inhibitor PKI had no effect. Data are mean ± S.E.M. of three independent experiments performed in duplicate. ***, $p < 0.001$; **, $p < 0.01$; Student-Newman-Keuls method for multiple comparisons after one-way ANOVA.

Using the rat injury model, the present study offers the first evidence demonstrating biological activity of BAY in attenuating vessel remodeling. The influence of BAY was observed only on neointimal growth and not on other vascular parameters, arguing against prolonged vasorelaxation or "outward remodeling" induced by BAY. These results corroborate earlier findings using the BAY prototype YC-1 (Tulis et al., 2002) and provide substantive evidence that pharmacologic sGC/cGMP agonism is a viable option in controlling vessel growth.

In the current study VSMC numbers were reduced by BAY, agreeing with our earlier report in A7R5 VSMCs (Mendelev et al., 2009). Using pharmacologic modulation of the respective NOS and HO pathways, the antiproliferative effects of BAY are believed to principally depend on upstream HO/CO signals and are not influenced by the NOS/NO pathway (Mendelev et al., 2009). In the current study, additional support for antimitogenic action of BAY was evident from flow cytometry in which BAY markedly (−70%) reduced cells in G_2/M. This static effect of BAY on VSM cell cycle progression parallels cell count data and provides sound explanation behind our observations that BAY inhibits growth through Cdk suppression and elevation in p21 and p27 (Mendelev et al., 2009). The G_2/M checkpoint is tightly regulated in part by the cyclin E/Cdk2 complex, whose activity increases during late G_2 and allows entry of cells into M. Moreover, the Cdk inhibitor p27 inhibits cyclin E/Cdk2 catalysis. Suppression of Cdk2 activity and elevation in p27 by BAY would retard movement of cells into the mitotic phase and reduce overall numbers in G_2/M, as observed. Furthermore, the Cdk inhibitor p21 is known to inhibit upstream cyclin D/Cdk4 signaling that is responsible for activation of essential E2F-responsive genes, and elevation in p21 by BAY could contribute to BAY-induced cytostasis. Cytotoxicity analysis reveals that BAY operates through pharmacological and not toxicological mechanisms, supporting our earlier observations (Mendelev et al., 2009).

Regarding migration, in the current study PKG inhibition completely reversed the antimigratory effects of BAY. Considering results demonstrating effectiveness with which DT-2 inhibits pVASPSer$_{239}$ in addition to PKG, these data provide sound evidence that BAY inhibits the migration of VSMCs through PKG-driven pVASPSer$_{239}$. The central role of VASP proteins in regulating cytoskeletal dynamics, along with recent findings showing that pVASPSer$_{239}$ controls remodeling of the actin skeleton during polymerization (Lund et al., 2010), offer ample evidence for the antimigratory effects of BAY through cGMP/PKG/pVASPSer$_{239}$.

In our earlier study (Mendelev at al., 2009) BAY doubled

cGMP and cAMP in A7R5 VSMCs. In the present study in primary VSMCs, cGMP stimulation was much more robust after BAY treatment. It is noteworthy that the earlier study used BAY at 0.001 μM, whereas the current study used BAY at 10 μM. In addition, both of these studies were performed in the presence of the broad phosphodiesterase (PDE) inhibitor IBMX, albeit at different concentrations and for different durations. In addition, differences in susceptibility toward BAY or other agents may be caused by phenotypic differences including sensitivities to exogenous stimuli between commercial and primary cells. It is noteworthy that in this study under identical conditions as those used to stimulate cGMP no further increases in cAMP were observed with BAY. This is rather surprising because cGMP has been shown to inhibit PDE3, which is responsible for cAMP metabolism (Maurice and Haslam, 1990). Conversely, it was recently shown that BAY can stimulate PDE3 expression in rat pulmonary VSM (Busch et al., 2010). In the current study it seems that IBMX is sufficient to maintain adequate basal levels of cAMP in primary VSM, after which further induction by BAY was not observed.

Stimulation of cGMP activates numerous downstream kinases that lead to specific phosphorylation cascades, and in VSM the primary effector of cGMP signaling is PKG. Another target of cGMP action in VSM is VASP, which plays key regulatory roles in cytoskeletal dynamics and migration. As mentioned, site-specific VASP phosphorylation can serve as a biomarker for kinase activation, with $pVASPSer_{157}$ indicative of PKA activity and $pVASPSer_{239}$ a marker for active PKG (Butt et al., 1994; Chen et al., 2004). However, other studies provide evidence for cross-talk between PKA and PKG and perhaps other kinases in mediating VASP phosphorylation (Smolenski et al., 1998; Chitaley et al., 2004), suggesting promiscuity in "site-specific" VASP phosphorylation. In the current study, BAY increased both $pVASPSer_{157}$ and $pVASPSer_{239}$. These findings differ slightly from that recently reported in a rat model of pulmonary hypertension (Thorsen et al., 2010) whereby BAY induced $pVASPSer_{239}$ yet failed to alter $pVASPSer_{157}$; however, that study was performed in lung homogenates under hypoxia, whereas the current study examined VSM under normoxia; thus, experimental conditions must be considered in cyclic nucleotide studies when using VASP as a "selective" kinase readout.

In the current study, pharmacologic kinase blockade showed that $pVASPSer_{239}$ is solely cGMP/PKG-driven because the PKG inhibitor DT-2 completely abolished this response. In comparison, elevation of $pVASPSer_{157}$, thought to be PKA-specific, was observed after BAY treatment albeit in the absence of detectable increases in cAMP. Moreover, the PKA-specific inhibitor PKI failed to reduce BAY-stimulated $pVASPSer_{157}$ and instead exaggerated this response. These findings are surprising but may be a further indication of cross-talk between cGMP and cAMP in terms of VASP phosphorylation. These events show that $pVASPSer_{157}$ can be elevated in the absence of cAMP and suggests that this phosphorylation site may involve alternate kinases (Chen et al., 2004) or PKA inhibition stimulates compensatory mechanisms leading to further increases in $pVASPSer_{157}$ and $pVASPSer_{239}$. Sequential and possibly allosteric activation of specific phosphorylation sites, with $pVASPSer_{239}$ preceding and inducing $pVASPSer_{157}$, is another possibility after BAY stimulation.

To investigate the mechanisms by which BAY contributes to growth suppression, specific kinase blockade was used in conjunction with BAY treatment. Earlier reports correlated increased $pVASPSer_{157}$ and $pVASPSer_{239}$ with inhibition of proliferation in rat primary VSMCs (Indolfi et al., 1997; Hewer et al., 2011). In agreement, in the current study BAY increased $pVASPSer_{157}$ and $pVASPSer_{239}$ and reduced VSMC proliferation. Moreover, in the presence of PKA inhibition, the antiproliferative ability of BAY was partially reversed, supporting a regulatory role for PKA in VSMC proliferation. A schematic showing our proposed antiproliferative and antimigratory actions of BAY in VSM is shown in Fig. 10.

It is noteworthy that with nonphosphorylatable VASP mutant VSMCs it has been suggested that $pVASPSer_{157}$ promotes whereas $pVASPSer_{239}$ inhibits proliferation (Chen et al., 2004). In separate studies we observed that low seeding densities reduce PKG expression, which may lend bias to studies examining cGMP signaling in VSMCs (Cornwell et al., 1994). In this study we plated 25,000 cells/well in 48-well plates for a maximum duration of 72 h, much higher densities and for shorter durations than that reported previously (Chen et al., 2004). In addition, preliminary data using pharmacologic blockade of sGC show that the action of BAY in primary VSM depends on an activated cyclase. Thrombospondin-1 and amyloid-β are increased in disease conditions including atherosclerosis, diabetes, and Alzheimer's disease and both serve as endogenous sGC inhibitors (Miller et al., 2010a,b). Moreover, the actions of BAY on sGC are more effective under reduced conditions (Jones et al., 2010), and in the setting of vascular disease or oxidative stress sGC may become oxidized and rendered less responsive to heme-dependent activation (Stasch et al., 2002). Accordingly, caution

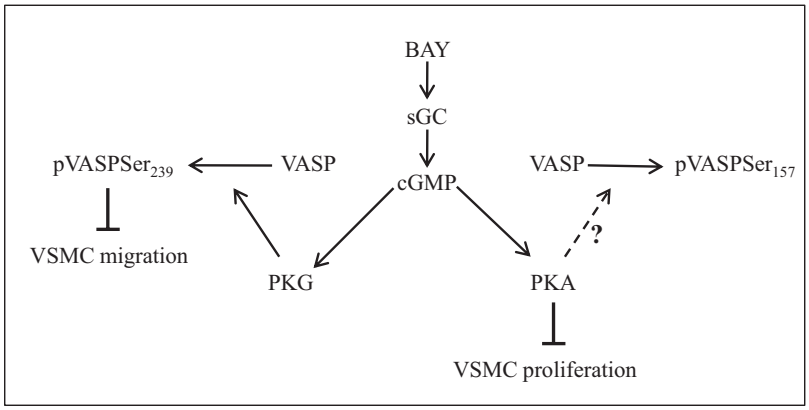

Fig. 10. Schematic showing the relationship between the functional end points proliferation and migration after pharmacologic induction of cGMP signaling by BAY. The antimigratory effects of BAY are mediated via PKG-$pVASPSer_{239}$, whereas the antiproliferative effects of BAY occur through PKA, yet do not necessarily involve $pVASPSer_{157}$.

must be used when designing cyclase-specific therapies under inimical conditions whereby endogenous cyclase inhibitors may be elevated and/or the enzyme rendered dysfunctional.

In conclusion, these findings support strategies targeting cGMP signaling in the control of VSM growth. In vivo and in vitro evidence is provided for the sGC stimulator BAY 41-2272, which effectively inhibits neointimal growth by reducing VSMC proliferation and migration through cGMP/PKA and cGMP/PKG/pVASPSer$_{239}$ signals, respectively. These data provide the initial evidence for BAY 41-2272 as an antigrowth regulator of VSM and offer support for continued study of its therapeutic potential.

Acknowledgments

We thank Drs. J. P. Stasch and A. Knorr (Bayer HealthCare AG, Berlin, Germany) for BAY 41-2272 and Dr. Shaquria P. Adderley (Brody School of Medicine, East Carolina University, Greenville, NC) for valuable discussions related to this work.

Authorship Contributions

Participated in research design: Joshi and Tulis.

Conducted experiments: Joshi, Martin, Fox, Mendelev, Brown, and Tulis.

Performed data analysis: Joshi and Tulis.

Wrote or contributed to the writing of the manuscript: Joshi and Tulis.

References

Boerrigter G, Costello-Boerrigter LC, Cataliotti A, Tsuruda T, Harty GJ, Lapp H, Stasch JP, and Burnett JC Jr (2003) Cardiorenal and humoral properties of a novel direct soluble guanylate cyclase stimulator BAY 41-2272 in experimental congestive heart failure. *Circulation* **107:**686–689.

Boerth NJ, Dey NB, Cornwell TL, and Lincoln TM (1997) Cyclic GMP-dependent protein kinase regulates vascular smooth muscle cell phenotype. *J Vasc Res* **34:**245–259.

Busch CJ, Graveline AR, Jiramongkolchai K, Liu H, Sanchez LS, and Bloch KD (2010) Phosphodiesterase 3A expression is modulated by nitric oxide in rat pulmonary artery smooth muscle cells. *J Physiol Pharmacol* **61:**663–669.

Butt E, Abel K, Krieger M, Palm D, Hoppe V, Hoppe J, and Walter U (1994) cAMP- and cGMP-dependent protein kinase phosphorylation sites of the focal adhesion vasodilator-stimulated phosphoprotein (VASP) in vitro and in intact human platelets. *J Biol Chem* **269:**14509–14517.

Chen H, Kovar J, Sissons S, Cox K, Matter W, Chadwell F, Luan P, Vlahos CJ, Schutz-Geschwender A, and Olive DM (2005) A cell-based immunocytochemical assay for monitoring kinase signaling pathways and drug efficacy. *Anal Biochem* **338:**136–142.

Chen L, Daum G, Chitaley K, Coats SA, Bowen-Pope DF, Eigenthaler M, Thumati NR, Walter U, and Clowes AW (2004) Vasodilator-stimulated phosphoprotein regulates proliferation and growth inhibition by nitric oxide in vascular smooth muscle cells. *Arterioscler Thromb Vasc Biol* **24:**1403–1408.

Chiche JD, Schlutsmeyer SM, Bloch DB, de la Monte SM, Roberts JD Jr, Filippov G, Janssens SP, Rosenzweig A, and Bloch KD (1998) Adenovirus-mediated gene transfer of cGMP-dependent protein kinase increases the sensitivity of cultured vascular smooth muscle cells to the antiproliferative and pro-apoptotic effects of nitric oxide/cGMP. *J Biol Chem* **273:**34263–34271.

Chitaley K, Chen L, Galler A, Walter U, Daum G, and Clowes AW (2004) Vasodilator-stimulated phosphoprotein is a substrate for protein kinase C. *FEBS Lett* **556:**211–215.

Cornwell TL, Soff GA, Traynor AE, and Lincoln TM (1994) Regulation of the expression of cyclic GMP-dependent protein kinase by cell density in vascular smooth muscle cells. *J Vasc Res* **31:**330–337.

Deguchi A, Soh JW, Li H, Pamukcu R, Thompson WJ, and Weinstein IB (2002) Vasodilator-stimulated phosphoprotein (VASP) phosphorylation provides a biomarker for the action of exisulind and related agents that activate protein kinase G. *Mol Cancer Ther* **1:**803–809.

Dey NB, Foley KF, Lincoln TM, and Dostmann WR (2005) Inhibition of cGMP-dependent protein kinase reverses phenotypic modulation of vascular smooth muscle cells. *J Cardiovasc Pharmacol* **45:**404–413.

Friebe A, Schultz G, and Koesling D (1996) Sensitizing soluble guanylyl cyclase to become a highly CO-sensitive enzyme. *EMBO J* **15:**6863–6868.

Han HJ, Heo JS, Lee YJ, Min JJ, and Park KS (2006) High glucose-induced inhibition of 2-deoxyglucose uptake is mediated by cAMP, protein kinase C, oxidative stress and mitogen-activated protein kinases in mouse embryonic stem cells. *Clin Exp Pharmacol Physiol* **33:**211–220.

Hewer RC, Sala-Newby GB, Wu YJ, Newby AC, and Bond M (2011) PKA and Epac synergistically inhibit smooth muscle cell proliferation. *J Mol Cell Cardiol* **50:** 87–98.

Indolfi C, Avvedimento EV, Di Lorenzo E, Esposito G, Rapacciuolo A, Giuliano P, Grieco D, Cavuto L, Stingone AM, Ciullo I, et al. (1997) Activation of cAMP-PKA signaling in vivo inhibits smooth muscle cell proliferation induced by vascular injury. *Nat Med* **3:**775–779.

Institute of Laboratory Animal Resources (1996) *Guide for the Care and Use of Laboratory Animals* 7th ed. Institute of Laboratory Animal Resources, Commission on Life Sciences, National Research Council, Washington DC.

Jones AW, Durante W, and Korthuis RJ (2010) Heme oxygenase-1 deficiency leads to alteration of soluble guanylate cyclase redox regulation. *J Pharmacol Exp Ther* **335:**85–91.

Koika V, Zhou Z, Vasileiadis I, Roussos C, Finetti F, Monti M, Morbidelli L, and Papapetropoulos A (2010) PKG-I inhibition attenuates vascular endothelial growth factor-stimulated angiogenesis. *Vascul Pharmacol* **53:**215–222.

Liu XM, Peyton KJ, Mendelev NN, Wang H, Tulis DA, and Durante W (2009) YC-1 stimulates the expression of gaseous monoxide-generating enzymes in vascular smooth muscle cells. *Mol Pharmacol* **75:**208–217.

Lund N, Henrion D, Tiede P, Ziche M, Schunkert H, and Ito WD (2010) Vimentin expression influences flow dependent VASP phosphorylation and regulates cell migration and proliferation. *Biochem Biophys Res Commun* **395:**401–406.

Maurice DH and Haslam RJ (1990) Molecular basis of the synergistic inhibition of platelet function by nitrovasodilators and activators of adenylate cyclase: inhibition of cyclic AMP breakdown by cyclic GMP. *Mol Pharmacol* **37:**671–681.

Mendelev NN, Williams VS, and Tulis DA (2009) Antigrowth properties of BAY 41-2272 in vascular smooth muscle cells. *J Cardiovasc Pharmacol* **53:**121–131.

Miller TW, Isenberg JS, and Roberts DD (2010a) Thrombospondin-1 is an inhibitor of pharmacological activation of soluble guanylate cyclase. *Br J Pharmacol* **159:** 1542–1547.

Miller TW, Isenberg JS, Shih HB, Wang Y, and Roberts DD (2010b) Amyloid-β inhibits No-cGMP signaling in a CD36- and CD47-dependent manner. *PloS ONE* **5:**e15686.

Profirovic J, Gorovoy M, Niu J, Pavlovic S, and Voyno-Yasenetskaya T (2005) A novel mechanism of G protein-dependent phosphorylation of vasodilator-stimulated phosphoprotein. *J Biol Chem* **280:**32866–32876.

Reinhard M, Jarchau T, and Walter U (2001) Actin-based motility: stop and go with Ena/VASP proteins. *Trends Biochem Sci* **26:**243–249.

Schlegel N and Waschke J (2009) VASP is involved in cAMP-mediated Rac 1 activation in microvascular endothelial cells. *Am J Physiol Cell Physiol* **296:**C453–C462.

Smolenski A, Bachmann C, Reinhard K, Hönig-Liedl P, Jarchau T, Hoschuetzky H, and Walter U (1998) Analysis and regulation of vasodilator-stimulated phosphoprotein serine 239 phosphorylation in vitro and in intact cells using a phosphospecific monoclonal antibody. *J Biol Chem* **273:**20029–20035.

Stasch JP, Schmidt P, Alonso-Alija C, Apeler H, Dembowsky K, Haerter M, Heil M, Minuth T, Perzborn E, Pleiss U, et al. (2002) NO- and haem-independent activation of soluble guanylyl cyclase: molecular basis and cardiovascular implications of a new pharmacological principle. *Br J Pharmacol* **136:**773–783.

Thorsen LB, Eskildsen-Helmond Y, Zibrandtsen H, Stasch JP, Simonsen U, and Laursen BE (2010) BAY 41-2272 inhibits the development of chronic hypoxia pulmonary hypertension in rats. *Eur J Pharmacol* **647:**147–154.

Tulis DA (2007a) Histological and morphometric analyses for rat carotid artery balloon injury studies. *Methods Mol Med* **139:**31–66.

Tulis DA (2007b) Rat carotid artery balloon injury model. *Methods Mol Med* **139:** 1–30.

Tulis DA, Bohl Masters KS, Lipke EA, Schiesser RL, Evans AJ, Peyton KJ, Durante W, West JL, and Schafer AI (2002) YC-1-mediated vascular protection through inhibition of smooth muscle cell proliferation and platelet function. *Biochem Biophys Res Commun* **291:**1014–1021.

Tulis DA, Durante W, Liu X, Evans AJ, Peyton KJ, and Schafer AI (2001) Adenovirus-mediated heme oxygenase-1 gene delivery inhibits injury-induced vascular neointima formation. *Circulation* **104:**2710–2715.

Wu CH, Chang WC, Chang GY, Kuo SC, and Teng CM (2004) The inhibitory mechanism of YC-1, a benzyl indazole, on smooth muscle cell proliferation: an in vitro and in vivo study. *J Pharmacol Sci* **94:**252–260.

Yang X, Thomas DP, Zhang X, Culver BW, Alexander BM, Murdoch WJ, Rao MN, Tulis DA, Ren J, and Sreejayan N (2006) Curcumin inhibits platelet-derived growth factor-stimulated vascular smooth muscle cell function and injury-induced neointima formation. *Arterioscler Thromb Vasc Biol* **26:**85–90.

Yonemoto W, Garrod SM, Bell SM, and Taylor SS (1993) Identification of phosphorylation sites in the recombinant catalytic subunit of cAMP-dependent protein kinase. *J Biol Chem* **268:**18626–18632.

Address correspondence to: Dr. David A. Tulis, Department of Physiology, Brody School of Medicine, East Carolina University, Greenville, NC 27834. E-mail: tulisd@ecu.edu